Type of presentation: Poster

MS-3-P-5702 Nanoanalytical investigations at the interface of 4H-SiC/SiO_2 MOSFETs

Tan H.[1], Beltran A. M.[1, 2], March K.[3], Mortet V.[2], Bedel-Pereira E.[2], Cristiano F.[2], Strenger C.[4], Bauer A. J.[4], Schamm-Chardon S.[1]

[1]CEMES-CNRS and Université de Toulouse, nMat group, Toulouse, France, [2]CNRS, LAAS, 7 avenue du colonel Roche, 31400 Toulouse, France, [3]Univ Paris 11, CNRS, UMR 8502, Lab Phys Solides, F-91405 Orsay, France , [4]Fraunhofer IISB, Schottkystrasse 10, 91058 Erlangen, Germany

Email of the presenting author: sylvie.schammchardon@cemes.fr

Despite the continuous improvement in performance and stability achieved in the development of 4H-SiC MOSFETs, the 4H-SiC MOS system still suffers from heavy carrier trapping at the SiO_2/SiC interface. It was proposed that interface states at the SiC/SiO_2 interface are responsible for the electron trapping but also bulk traps in SiC[1]. Furthermore it was suggested that the density of these bulk traps is significantly increased by ion implantation followed by high-temperature anneals. At the same time several groups provided experimental evidence for a carbon rich transition region on the SiC side of the interface with a C/Si ratio higher than one, and even, the width of the carbon-rich transition region was found inversely related to the peak field effect mobility[2]. It was also proposed that C di-interstitial defects in the SiC side of the interface account for the increased bulk trap density in SiC[3].

In this work, differently processed n-channel planar MOSFETs manufactured on p-implanted n-type 4H-SiC epitaxial layers are considered. In particular, the effect of different channel implantation concentrations is examined. We have investigated the structural and chemical state of these MOSFETs focusing on the structural state and C distribution at the interface using high resolution scanning transmission electron microscopy (HR-STEM) (0.1 nm) and spatially resolved electron energy loss spectroscopy (STEM-EELS). The *Si-L* edge (100 eV), *C-K* edge (284 eV) and *O-K* edge (532eV) were collected in the same spectrum. The n-channel MOSFETs were investigated after FIB sample preparation.

Based on the relative compositions extracted from our EELS data, no C excess is evidenced for the samples neither in the SiC substrate nor in the SiO_2 gate oxide. However, modification of the *Si-L* ELNES was revealed and numerically exploited. In particular, fitting of the *Si-L* edge evolution across the interface with a linear combination of reference spectra (Si, SiC and SiO_2) evidences the presence of a « suboxide » over a short distance (less than 2 nm) at the SiC/SiO_2 interface. It implies a transition layer where the Si bonding is modified compared to what is observed either in SiC or in SiO_2. These results will be commented with regard to electron mobility measurements[4].

1. A Agarwal, S Haney, J. Elec. Mater 37, 646 (2008)

2. T.L.Biggerstaff et al., Appl. Phys. Lett. 95, 032108 (2009)

3. X. Shen et al., Appl. Phys. Lett. 98, 053507 (2011)

4. A. M. Beltran et al., Materials Science Forum 711, 134 (2012)

* A.M. Beltran now at CENEM, Universität Erlangen-Nürnberg, Erlangen, Germany

Acknowledgement: Work performed by the French-German Consortium MobiSiC, supported by the Programme Inter Carnot Fraunhofer from BMBF (G.A.312483). Thanks to the French METSA network for the access to the probe-corrected Ultra-STEM Nion microscope, Orsay, France.

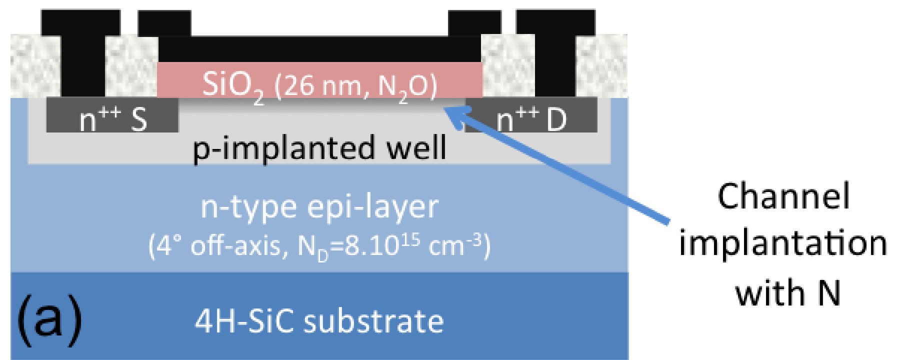

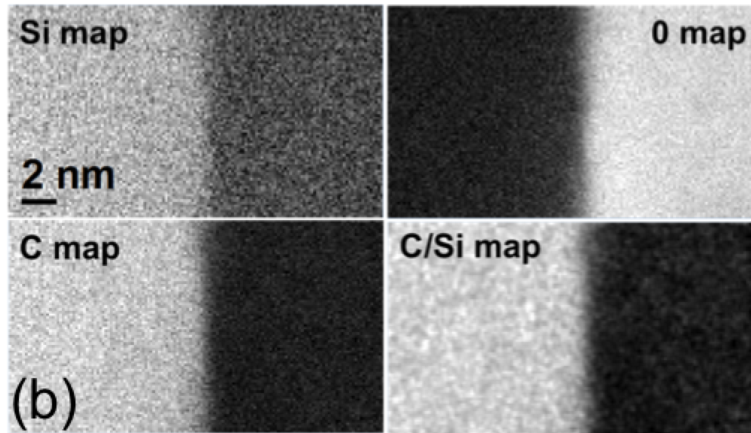

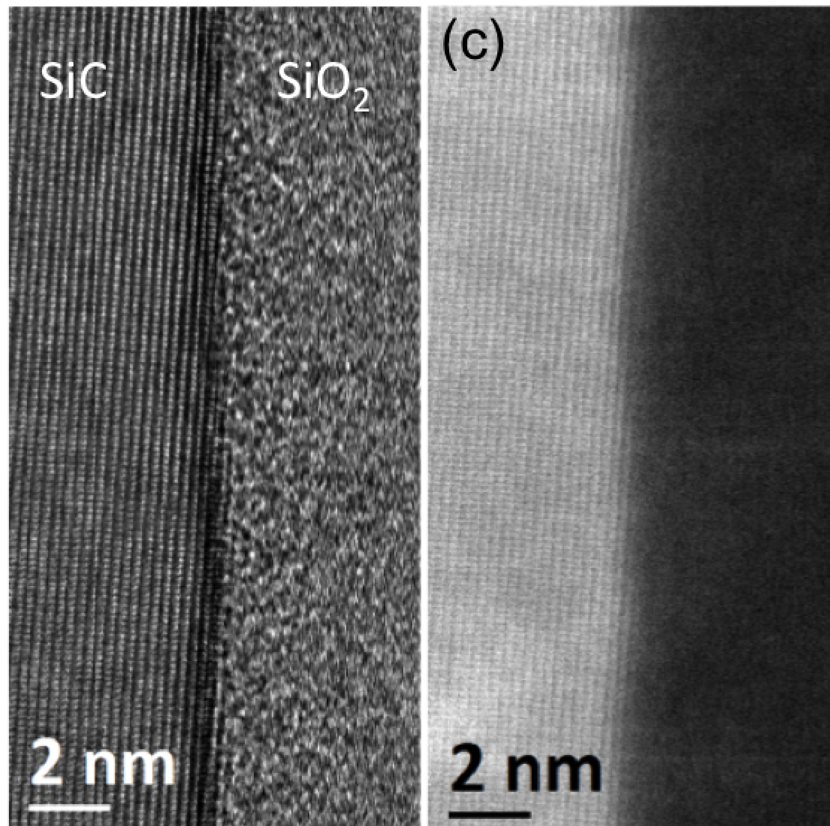

Fig. 1: (a) Schematic cross-section of the studied MOSFETs; (b) STEM-EELS elemental maps across one 4H-SiC/SiO_2 interface and the corresponding C/Si ratio map; (c) STEM Bright-field (left) and STEM-HAADF (right) images across one 4H-SiC/SiO_2 interface.

LS-4-P-2882 Three-dimensional reconstruction of the S885A mutant of the human mitochondrial Lon protease

Belmonte M.

MS-2-P-3370 Novel 3-dimensional nanocomposite of covalently interconnected multiwalled carbon nanotubes using Silicon as an atomic welder

Belovari T.

LS-13-P-2014 Presence of Trefoil factor 1, 2 and 3 in the embryonal epidermis of a mouse

Beltowska-Lehman E.

MS-4-P-3421 Transmission electron microscopy and X-ray diffraction studies of Ni-W/ZrO_2 metal-matrix composites

Beltran A. M.

MS-3-P-5702 Nanoanalytical investigations at the interface of 4H-SiC/SiO_2 MOSFETs

Beltrán A. M.

IT-10-P-2637 Combined 3D characterization of porous zeolites by STEM and FIB tomography

Bemis J.

MS-6-P-5979 AM-FM and Loss Tangent Imaging – New Tools for Quantitative Nanomechanical Properties

Ben Jemaa N.

LS-2-P-2215 Gadolinium in the lactating mammary gland tissue. Ultrastructural and microanalytical study

Benabbas C.

MS-10-P-3453 Morphological and chemical characterization of sandstone from Constantine, North-East of Algeria.

MS-13-P-3471 A multi-technique approach by SEM/EDS, Optical Microscopy, XRD, FT-IR to characterize limestone from Constantine, North-East of Algeria.

Benada J.

ID-4-P-3235 High-content microscopy screening to identify novel chemical compounds modulating DNA damage response

Benada O.

ID-2-P-3535 Sample damage during MALDI MS imaging and its impact on MSI lateral resolution

Benaissa M.

MS-1-O-2203 Plasmon energy from strained GaN quantum wells

Benchimol M.

LS-7-P-1769 Behavior of the Lysosome related organelle during differentiation of Giardia intestinalis

LS-7-P-2489 Mitosome behavior during the life cycle of the pathogenic protozoan Giardia intestinalis

Benckiser E.

IT-2-P-1751 The atomic structure of epitaxially strained $LaNiO_3$-$LaGaO_3$ superlattices

Bender H.

MS-8-O-1702 Investigation of 3D Strain in FinFETs by Nano Beam Diffraction Parallel and Perpendicular to the Trenches

MS-8-P-3339 TEM analysis and electrical probing on thin TEM lamellas of CBRAM stacks

IT-10-P-5857 3D imaging of Si FinFETs by combined HAADF-STEM and EDS tomography

Benecke M.